A Two Concentric Slot Loop Based Connected Array MIMO Antenna System for 4G/5G Terminals

A Two Concentric Slot Loop Based Connected Array MIMO Antenna System for 4G/5G Terminals

Mohammad S. Sharawi, Muhammad Ikram and Atif Shamim

Abstract- In this work, an integrated design with multiple-input multiple-output (MIMO) antenna system for 4G and 5G applications is presented. The proposed design contains a 2-element slot based MIMO antenna system for 4G and a connected antenna array (CAA) based 2-element MIMO antenna system for a potential 5G band. Two rectangular loops are etched on the periphery of the ground plane. The top and bottom portions of the thin loops act as the two 4G MIMO antennas, while parts of their sides are acting as 5G arrays. The antenna system is fabricated on a commercially available Roger 4350 substrate with ϵ_r equal to 3.5 while the dimensions of the board are $100\times60\times0.76$ mm^3 representing a typical smart phone back plane size. The integrated antenna system covers multi-bands at 4G with a combined bandwidth of 1.565 GHz (-6dB BW) in addition to the band between 16.50-17.80 GHz for 5G. The design is planar, low profile, simple and compact in structure making suitable for wireless handheld devices and mobile terminals. The measured gain at 3.46 GHz was at least 2.22 dBi and at 17 Ghz was 8 dBi for the 4G and 5G MIMO antenna systems, respectively. The Envelope correlation coefficient (ECC) was also calculated from the measured 3D patterns and showed good MIMO performance. This is the first integrated 4G/5G MIMO antenna system with below 6 GHz and above 10 Ghz covered bands using CAA.

Keywords: Connected antenna arrays, MIMO, isolation, 4G/5G.

I. Introduction

To be able to satisfy the continuous increased demand in data rate requirements in future communication systems, Multiple-input multiple-output (MIMO) technology with wider bandwidth should be used hand in hand with other enabling ones. MIMO systems can increase the data rate within limited power and bandwidth [1]. They are currently used in the fourth generation (4G) mobile phones and will also be used in fifth generation (5G) one with higher number of antennas at higher frequency bands. Utilizing higher frequency bands (i. e. at millimeter waves) with wider bandwidth provides high data rates. Therefore, to design small size multiple antennas with wide bandwidths and covering multiple bands within a mobile phone is a hot topic for antenna designers [2].

PIFA and monopole based MIMO antennas are famous for mobile applications due to their compact size and ease of fabrication. A 4-element PIFA based MIMO antenna system was reported in [3] for LTE applications. It covered 1.84-2.69 GHz band. The board dimensions were $136\times68.8\times6$ mm^3. Minimum isolation reported was 14.2dB. Another design with 8-element MIMO antenna system was reported in [4]. It was covering two bands from 2.6-2.8 GHz and 3.4-3.6 GHz. The overall board size was $140\times70\times9.55$ mm^3. They have improved isolation using separate ground planes.

A monopole based MIMO antenna system with multi-band capability was presented in [5]. It was covering 0.7, 1.7, 2.1, 2.3 and 2.5 GHz frequency bands. Separate ground planes were used to improve an isolation upto 13 dB. The overall board size was 153×83 mm^2. In [6], 2-element printed monopole MIMO antenna system was reported. The board dimensions were 125×85 mm^2. Isolation was improved using defected ground structure. In [7], a 4-element monopole based MIMO antenna system was presented. The overall size of the board was 150×150 mm^2. It was multi-band antenna system covering frequency bands between 699-798 MHz, 1.7-2.0 GHz and 2.3-2.5 GHz. Multiple resonances were achieved using different set of antennas. Finally, a 4-element monopole based MIMO antenna system was reported in [8] with the board dimensions of 110×110 mm^2. It covered the frequency bands 1.95 GHz, 2.39 GHz, 2.64 GHz and 3.27 GHz.

Connected antenna arrays (CAA) are used due to their wide-band and wide scan properties [9]-[11]. The operating principles of slot based CAA were reported in [9] while [10] discussed array scanning properties. A wide-band CAA based on dipole elements was reported in [11]. It was operating between 3 to 5 GHz. A 7×7 prototype of the CAA was presented. The total size of the array was 15.2×21.6 cm^2. A similar CAA design was presented in [12]. A new feeding network was designed to suppress common mode resonances. It was covering the 450-1450 MHz frequency band. All of the above works related to CAA were presented for radar applications.

A recent design for broadband cellular communications was presented in [13]. It was based on a linear CAA of a single long slot which was fed from three points using a reactively matched feeding structure that operated at 1.74, 2.55 and 3.4 GHz. The total size of the board was 235×118 mm^2 with a slot size of 1.8×71 mm^2. Furthermore, a long slot based CAA was reported in [14] for phased array applications. It operated at 0.4-2 GHz band. It consisted of 15×15 elements.

For 5G applications, some work has been done in mm-wave range. In [15], a 4-element array for MIMO applications was presented. It operated at 30GHz. Isolation was improved using a separate ground plane for each element. Other mm wave antenna systems at 28GHz were presented in [16], [17] for 5G applications. A 4G/5G MIMO antenna system with board dimensions $170\times70\times0.8$ mm^3 was presented in [18]. It was

M. S. Sharawi and M. Ikram are with the Electrical Engineering Department, King Fahd University for Petroleum and Minerals (KFUPM), Dhahran, 31261 Saudi Arabia, Email: {*msharawi, g201409500*}*@kfupm.edu.sa*

A. Shamim is with Computer, Electrical and Mathematical Sciences and Engineering Division, King Abdullah University Of Science & Technology (KAUST), Saudi Arabia, Email: *atif.shamim@kaust.edu.sa*

This work was supported by The Deanship of Scientific Research (DSR) at KFUPM under project no. RG1423.

covering multiple bands (900, 1800, 2100, 2300 MHz for 4G and 3400-3600 MHz for 5G). In [19], 8-element PIFA based MIMO antenna system was presented for 5G mobile phones. The MIMO system was operating at GSM (1900 MHz), LTE (2300 and 2500 MHz) bands. The overall size of the board was $136\times68.8\times1$ mm^3.

From the above discussion, MIMO antenna systems were reported in [3]-[8] based on PIFA and monopole elements. Most of them were used for 4G applications. Connected arrays were reported in [9]-[14] for wide-band applications. Almost all of the works were implemented on a large substrate size that can not fit within mobile handheld devices. In [15]-[17], mm-wave arrays were presented for 5G applications while [18]-[19] showed sub-6GHz MIMO antenna systems for 5G. No work has been done for an integrated design covering 4G/5G for mobile phones where the 4G MIMO antenna system covers microwave ranges and the 5G MIMO antenna system covers above 6 GHz wide bands, with minimum size and simple structure and utilizing CAA.

In this work, a novel integrated 4G/5G MIMO antenna system is presented using the concept of CAA. Two slots are etched on the periphery of the ground plane and act as the radiating structure for all subsequent antennas. The proposed design consists of a 2-element slot based MIMO antenna system for 4G and a 2-element MIMO antenna array for 5G. It is a multi-band MIMO antenna system that covers 1975-3540 MHz with a minimum bandwidth of 1.565 GHz (-6dB BW), and 16.50-17.80 GHz band with 1.3 GHz measured bandwidth (-10dB BW) for 5G. The design is planar, low profile, simple with compact structure that is suitable for wireless handheld devices and mobile terminals. MIMO performance metrics were calculated to show good MIMO operation.

II. Design of the Integrated 4G/5G Antenna System

The geometry of the proposed antenna system is shown in Fig. 1. It consists of two MIMO antenna systems, one covering 4G bands and the other covers a potential 5G band. It is modeled and simulated using CST Microwave studio ver. 2015.

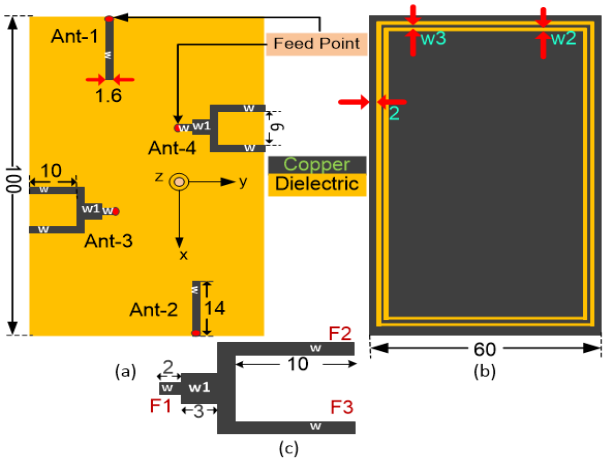

Fig. 1: Proposed integrated CAA based MIMO antenna system design (a) Top view (b) Bottom view (c) Feed network for the CAA- All dimensions are in millimeters (mm).

An RO4350 material with a dielectric constant (ϵ_r) of 3.5 and height of 0.76mm is used as a substrate. The overall board dimensions are $100\times60\times0.76$ mm^3. The top layer (Fig. 1(a)) shows the feeding structures for the various antenna elements and their port locations, while the bottom layer shows the system ground plane with two concentric rectangular thin slot loops along its periphery.

The 4G MIMO antenna system consists of two elements ANT-1 and ANT-2. Each of the two 4G antenna feeding arms are exciting two slots underneath to act as a slot antenna. The 5G MIMO antenna system uses a 1×2 antenna array for each port (ANT-3 and ANT-4), utilizing power combiners/dividers to excite them. Each array consist of two-elements in each, as each combiner is a two-to-one structure with two slots being excited on the GND plane with quarter guided wavelength design at the desired frequency of operation. The excited slots are in a CAA configuration for compact design and wide operating bandwidth.

The design process goes through two steps; one for the 4G MIMO part and the second for the 5G array one.

A. Step 1: 4G MIMO design

Two slots are etched on the periphery of the GND plane, 4mm away from the edge of the substrate. Two microstrip lines (Ant-1 & Ant-2) on the top and bottom edges are used to excite the slots acting as two slot antennas as shown in the Fig. 1(a). The length and width of these feed lines are 20mm and 1.6mm, respectively. The location and length of the feeds are optimized along the y-axis to match with 50 Ω. We can achieve resonance in the band of interest by changing the location of feed lines and the spacing between the slots ($w3$) in addition to their width ($w2$). The parametric analysis is shown in Fig. 2(a) and Fig. 2(b) by changing $w3$ and $w2$, respectively.

Multiple resonances were achieved by this configuration with wide bandwidth. Fig. 2(c) shows the reflection coefficients of the optimized 4G MIMO antenna system with $w2$=1mm, $w3$=2mm. It is covering 1978-2260, 2450-2521, 2690-3050 and 3250-3630 MHz with 282, 71, 360 and 380 MHz bandwidths (-10dB bandwidth) while the -6dB bandwidth is 700 MHz (1.7-2.4), 850 MHz (2.45-3.3 GHz) and 650 MHz (3.35-4 GHz) within the bands covered. Fig. 2(d) shows the isolation between Ant-1 and Ant-2. Isolation is poor which is expected because the two antennas are directly connected. This is a known feature of CAA [9]-[11].

B. Step 2: 5G CAA MIMO design

For the 5G MIMO system, we need two arrays. The arrays consist of 1×2 connected ones (more elements can be used, but a 1×2 is used as a proof of concept). The array of slots is used to increase the gain as compared to a single slot. Each array is activated by two-to-one power divider/combiner. The power divider/combiner is designed and optimized at the band of interest. The length of each arm (F2 and F3) is 15.8mm and the spacing between them is 8mm. The widths of F1-F3 and w microstrip-lines are 1.6mm to give 50 Ω lines while $w1$ widths are set to 3mm to provide 35 Ω $\lambda/4$ transformers.

These transformers are used to convert 25 Ω to 50 Ω. In this configuration, the spacing between the feed arms (F2 and F3) and the location of feed lines (along x and y axis) are the main parameters to achieve the resonance at the band of interest.
The simulated reflection coefficients are shown in Fig. 3(a) and 3(c) for the lower (4G) and higher (5G) bands. It is covering 1900-2250, 2300-2500 and 3350-3900 MHz (-6dB BW) for the lower bands and 12.90-16.00 GHz (-10dB BW) for higher band with 350, 200, 550 MHz and 3.1 GHz bandwidths, respectively. Isolation curves for the lower bands are shown in Fig. 3(b) and for the higher band are shown in Fig. 3(d). Only at the lower bands (4G) isolation between Ant-1 and Ant-2 is low because in CAA, elements are connected to each other with large wavelength and suffer from low isolation [11]. At higher bands, isolation is more than 10dB which is an acceptable value for mobile applications.

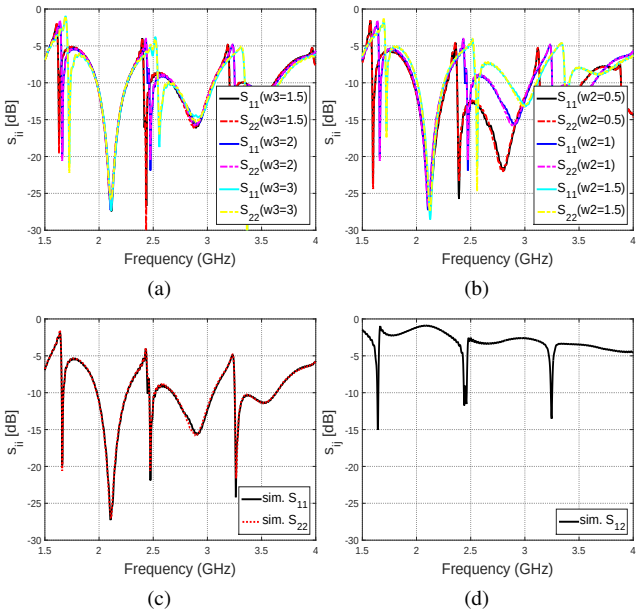

Fig. 2: S-parameters curves with only the 4G MIMO antenna system (a) $|s_{ii}|$-Simulated for different values of $w3$ (b) $|s_{ii}|$-Simulated for different values of $w2$ (c) $|s_{ii}|$-Simulated with $w2$=1mm & $w3$=2mm (d) $|s_{ij}|$-Simulated.

C. Optimized 4G/5G MIMO Antenna Design

After the study of the various effects, we were able to implement an optimized design. The optimized values were, the spacing between slots ($w3$) is 0.5mm, slot width ($w2$) is 0.6mm, slot distance from the edge of the board is only 2mm, the length of F1-F2 is 10mm, the length of the feed lines for the 4G MIMO is 14mm. The optimized feed network is simulated alone to give equal magnitude and similar phase. The magnitude and phase curves of the transmission coefficients between F1 (input of the CAA as shown in Fig. 1(c)) to F2-F3 (excitation ports of the CAA) are shown in Fig. 4(a) and Fig.4(b), respectively. After optimization, the bandwidth was decreased a little but still can fulfill the requirements for 5G applications.
The current distributions are shown in Fig. 5 at different frequencies showing the behavior of both antenna systems. In Fig. 5(a) and Fig. 5(b), P1 and P2 are activated at 2.1 GHz, respectively and others are terminated with matched load. High coupling current is observed between P1 and P2. In Fig. 5(c) and Fig. 5(d), P3 (Ant-3) and P4 (Ant-4) are activated at 17 GHz, respectively, while others are terminated with matched loads. Lower coupling currents are observed at the higher band as the inactive ports lie within a current minima.

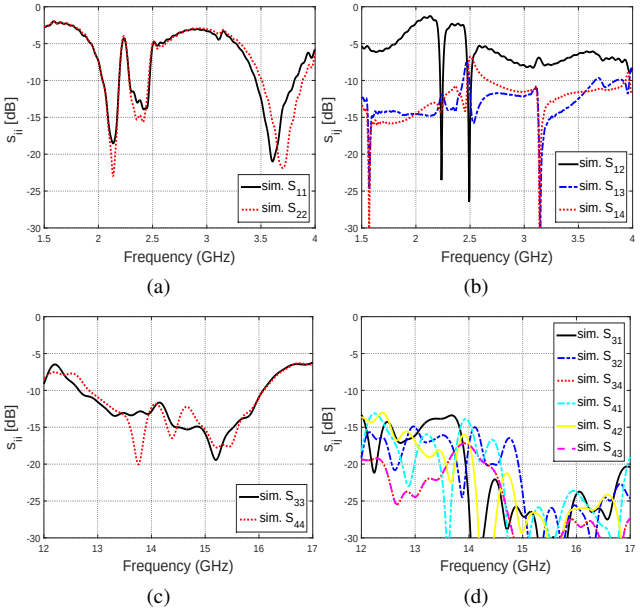

Fig. 3: S-parameters curves of the integrated design without optimization (a) $|s_{ii}|$-Simulated for lower bands (b) $|s_{ij}|$-Simulated for lower bands (c) $|s_{ii}|$-Simulated for higher band (d) $|s_{ij}|$-Simulated for higher band, {simulated (sim.), measured(mea.)}.

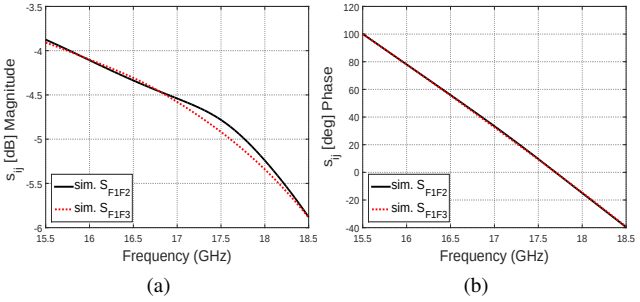

Fig. 4: Transmission coefficient curves of the feed network alone (a) $|s_{ij}|$-Simulated magnitude (b) $|s_{ij}|$-Simulated phase.

III. Results and Discussions

The fabricated prototype was made using an LPKF S103 milling machine at KFUPM. The S-parameters of the fabricated design were measured using an Agilent N9918A vector network analyzer. The radiation patterns and efficiency were measured using a SATIMO star lab chamber at MVG-Italy. The fabricated prototype is shown in Fig. 6. The measurement setup is shown in Fig. 7.

A. Port Parameters

The simulated and measured reflection coefficient curves of the proposed design for the 4G MIMO system part are shown in Fig. 8(a). All the resonance curves show that the 2-elements of the 4G MIMO antenna system are resonating at multiple-bands. The measured minimum -10dB bandwidth was 105 MHz from 1975 to 2080 MHz, 70 MHz from 2160 to 2230 MHz, 270 MHz from 2350 to 2620 MHz, 80 MHz from 3060 to 3140 MHz and 60 MHz from 3480 to 3540 MHz while the minimum -6dB bandwidth was 177 MHz from 1948 to 2125 MHz, 640 MHz from 2150 to 2790 MHz, 319 MHz from 2836 to 3155 MHz, 124 MHz from 3436 to 3560 MHz and 342 MHz from 3598 to 3940 MHz. Fig. 8(c) shows the simulated and measured reflection coefficient curves of the proposed design for the 5G MIMO antenna system part. The measured minimum -10dB bandwidth was 1.3GHz from 16.50 to 17.80 GHz and -6dB bandwidth was 2.7GHz from 15.8 to 18.5 GHz.

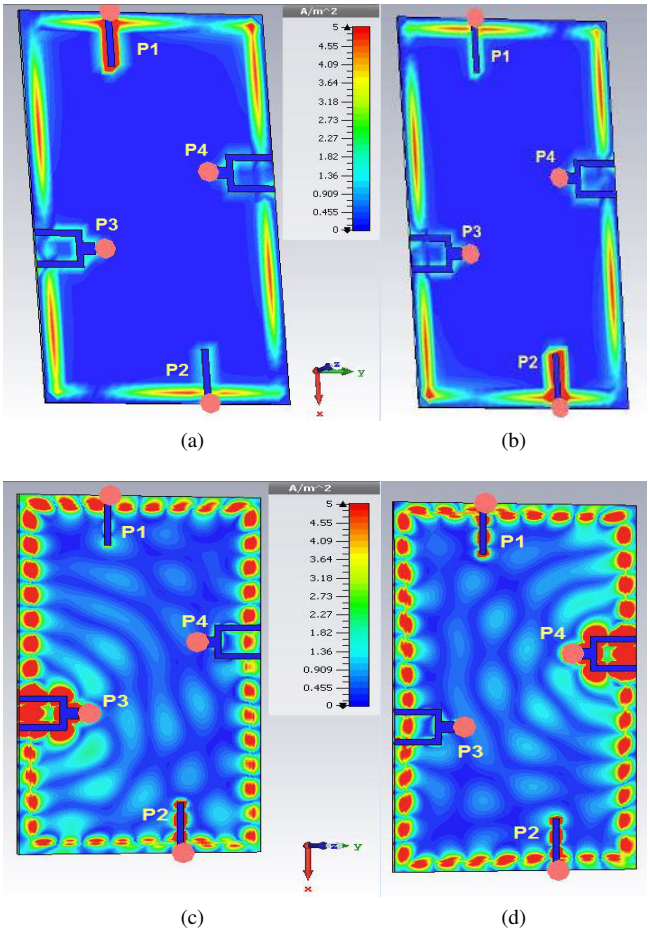

Fig. 5: Current distributions on the proposed design (a) P1 at 2.1 GHz is activated (b) P2 is activated at 2.1 GHz (c) P3 is activated at 17 GHz (d) P4 is activated at 17 GHz.

The simulated and measured isolation curves of the proposed design at 4G bands and 5G bands are shown in Figs. 8(b) and 8(d), respectively. The minimum measured isolation at the lower band was 4dB between Ant-1 and Ant-2 and more than 10dB between all other elements. A good agreement between simulated and measured results is observed.

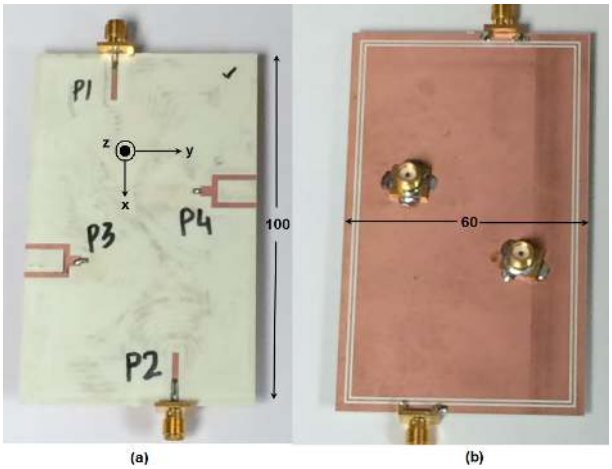

Fig. 6: Fabricated model of integrated design (a) Top view (b) Bottom view - All dimensions are in millimeters (mm).

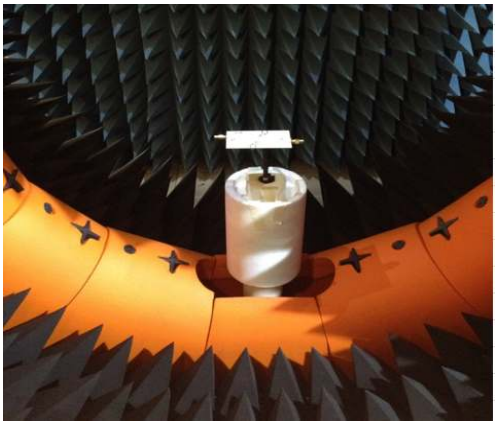

Fig. 7: The Proposed antenna design in the measurement setup in a Satimo star chamber.

B. Radiation Patterns

Simulated 3D gain patterns are shown in Fig. 9. The Figs. 9(a) and 9(b) are showing gain values for the 4G MIMO antenna system for Ant-1 and Ant-2 at 2.1 GHz, respectively. The maximum value of gain is 3 dBi. For the 5G MIMO antenna system, gain values are shown in Figs. 9(c) and 9(d) for Ant-3 and Ant-4, respectively. The maximum gain value is 8.23 dBi at 17 GHz.

The simulated and measured normalized 2D radiation patterns in terms of the total E-filed ($Etotal$) for the 4G/5G integrated design are illustrated in Fig. 10 for the x-y and y-z planes (referred to Fig. 1). The maximum measured values of $Etotal$ for Ant-1 ant Ant-2 were 0.5818 dB, 0.0016 dB, respectively while it was 4.19 dB for Ant-3 and Ant-4, respectively. In Figs. 10(a) and 10(c), 2-D $\theta - cuts$ are plotted for each antenna at $\phi = 0^o$. In Figs. 10(b) and 10(d), 2-D $\phi - cuts$ at $\theta = 90^o$ for

each antennas are shown. The beams are tilted showing low correlation and good MIMO performances.

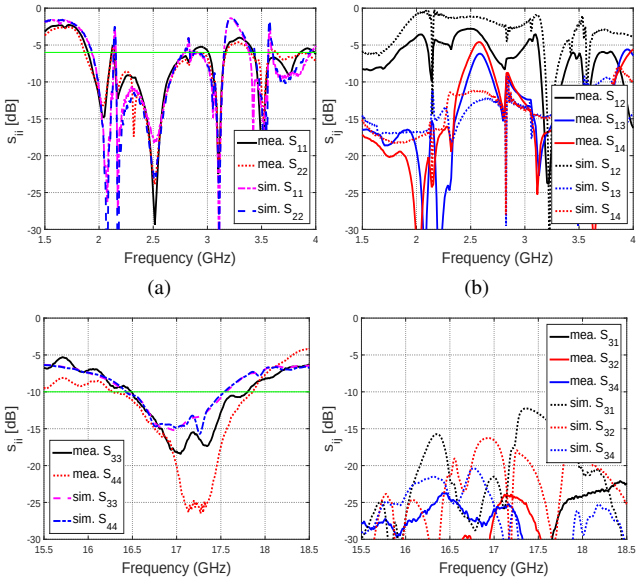

Fig. 8: S-parameters curves without DGS (a) $|s_{ii}|$-Simulated (b) $|s_{ii}|$-Measured (c) $|s_{ij}|$-Simulated (d) $|s_{ij}|$-Measured, {simulated (sim.), measured(mea.)}.

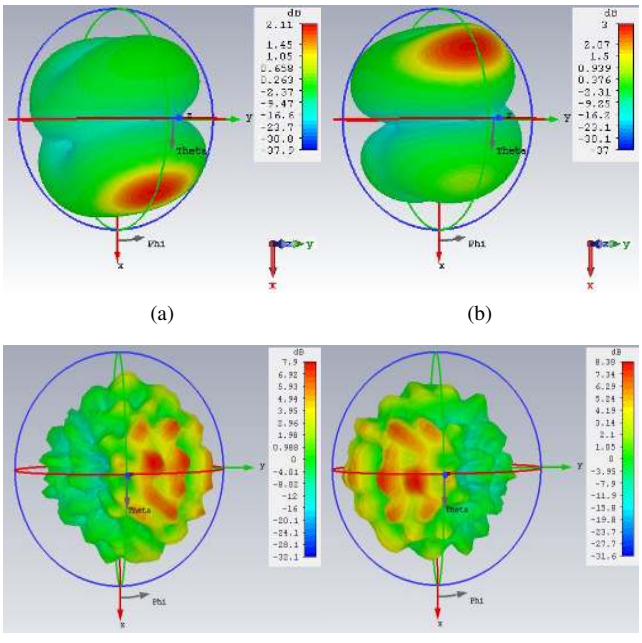

Fig. 9: Gain patterns (a) Ant-1 is activated at 2.1 GHz (b) Ant-2 is activated at 2.1 GHz (c) Ant-3 is activated at 17 GHz (d) Ant-4 is activated at 17 GHz.

The measured maximum gain and efficiency values of Ant-1 and Ant-2 are shown in Fig. 11(a) and 11(b) respectively. The minimum efficiency was 27% at 2.45 GHz. The curves of maximum gain and efficiency versus frequency for Ant-3 and Ant-4 are shown in Fig. 11(c) and 11(d), respectively. The minimum efficiency value was 80% at 17.3 GHz.

C. MIMO Performance

The envelope correlation coefficient (ECC) is a MIMO performance metric which is used to evaluate diversity performance. ECC values were computed based on the measured 3D radiation patterns [1]. The maximum obtained value of 0.3585 was between Ant-1 and Ant-2 at 2.5 GHz while, it was 0.0538 between Ant-3 and Ant-4 at 17.5 GHz. At other frequencies the values of the measured ECC for 4G bands are given in Table I while Table II shows ECC values for the 5G band. All values are below 0.5 that shows that this proposed integrated design can fulfill the requirements of a 4G/5G MIMO antenna system.

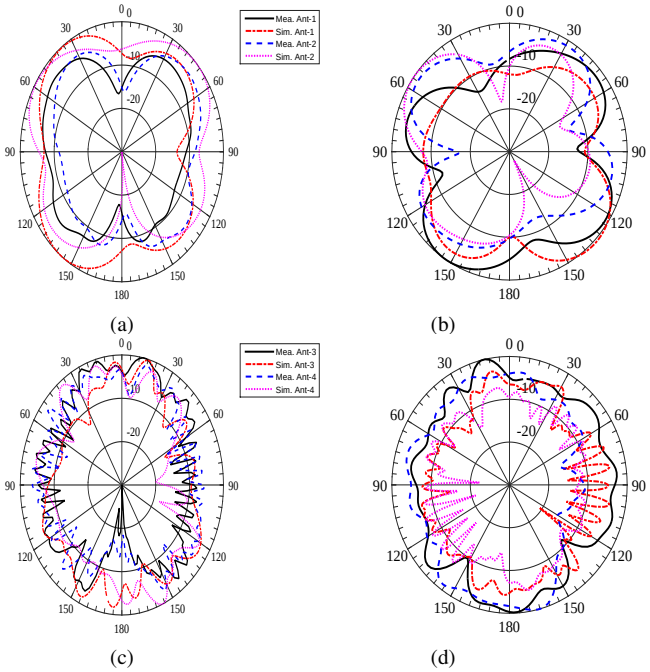

Fig. 10: Measured and simulated normalized radiation patterns (E_{total}) (a) $(\theta-cuts)$ Ant-1 and Ant-2 at $\phi = 0^o$ (b) $(\phi-cuts)$ Ant-1 and Ant-2 at $\theta = 90^o$ (c) $(\theta - cuts)$ Ant-3 and Ant-4 at $\phi = 0^o$ (d) $(\phi - cuts)$ Ant-3 and Ant-4 at $\theta = 90^o$.

D. Isolation Enhancement Structure

To improve the port isolation between the ports of the CAA, an isolation enhancement structure based on 4-loops is used as shown in Fig. 12. It is based on a defected ground structure (DGS) working as a band reject filter in the 4G bands. The width and length of each loop are optimized to 7.5mm and 20mm, respectively. This is just one method to enhance port isolation with minimum effect on other parameters. The fabricated model of the proposed design with the isolation enhancement structure is shown in Fig. 13.
The measured and simulated S-parameter curves of the proposed design with DGS only for the 4G MIMO antenna system are shown in Fig. 14 because isolation improvement

was needed in these bands. The covered bands are 2070-2290, 2350-2460, 2720-3050 and 3530-4000 GHz with -6dB bandwidth of 220, 110, 330 and 470 MHz, respectively. Isolation curves are shown in Fig. 14(b). It is observed that more than 10dB of isolation is obtained in all bands. At least 6dB improvement is obtained. Only in the 3530-4000 MHz band, there was no improvement observed. Isolation improvement can also be seen if we compare Fig. 8(b) and Fig. 14(b).

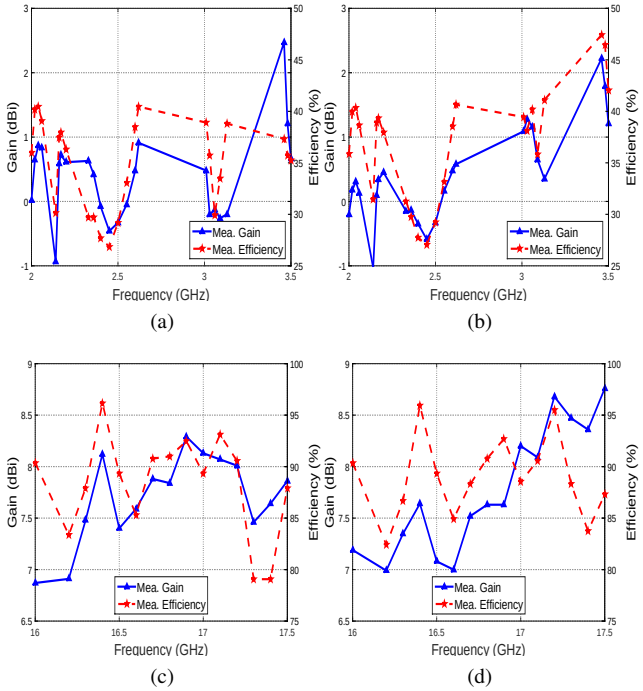

Fig. 11: Measured gain and efficiency (a) Ant-1 (b) Ant-2 (c) Ant-3 (d) Ant-4.

Isolation improvement can also be seen from the current distribution as shown in Fig. 15. In Figs. 15(a) and 15(b), P1 and P3 are activated, respectively and others are terminated with matched loads. The current is traped in the DGS reducing the coupling currents.

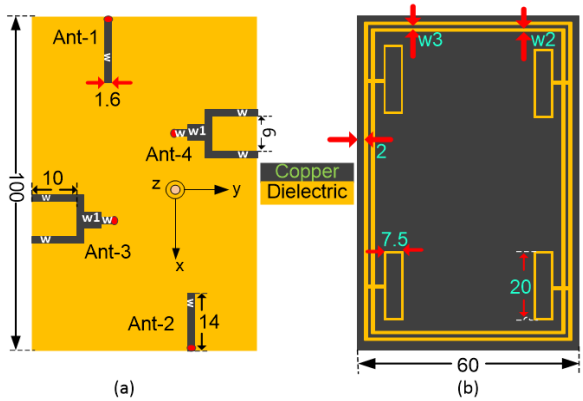

Fig. 12: Proposed integrated CAA based MIMO antenna system design with isolation enhancement structure (a) Top view (b) Bottom view- All dimensions are in millimeters (mm).

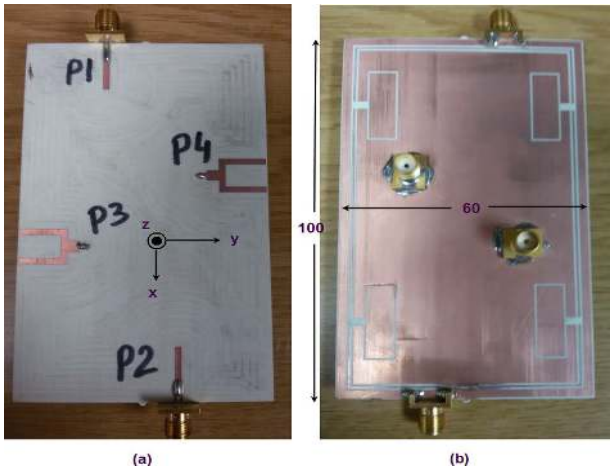

Fig. 13: Fabricated model of integrated design with isolation enhancement structure (a) Top view (b) Bottom view - All dimensions are in millimeters (mm).

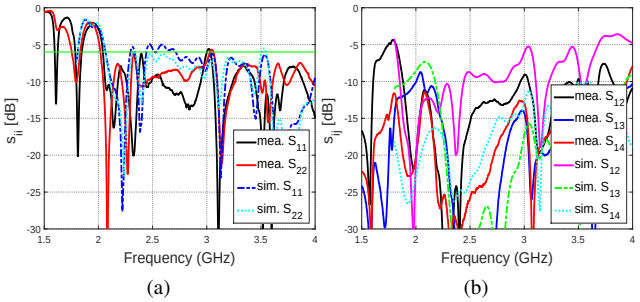

Fig. 14: S-parameter curves with DGS (a) $|s_{ii}|$-Measured and simulated (b) $|s_{ij}|$-Measured and simulated.

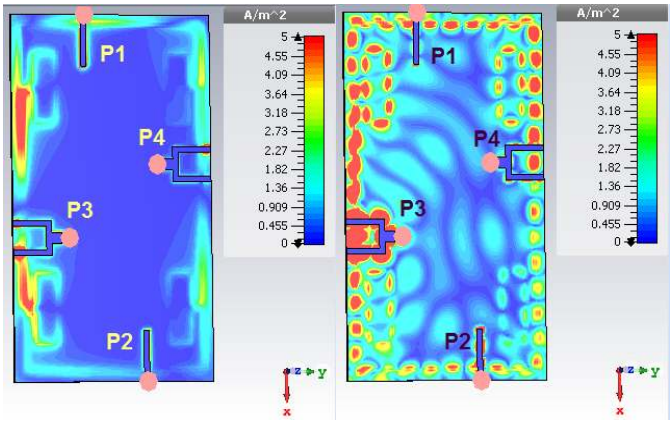

Fig. 15: Current distributions on the proposed design with isolation enhancement structure (a) P1 at 2.1 GHz is activated (b) P3 is activated at 17 GHz.

TABLE I: Measured envelope correlation coefficient (ECC) values for 4G bands.

Freq	2.02	2.14	2.4	2.5	3.5
ECC12	0.0384	0.0001	0.1843	0.3585	0.0451

TABLE II: Measured envelope correlation coefficient (ECC) values for 5G band.

Freq	16.5	16.7	17	17.2	17.5
ECC34	0.0180	0.0219	0.0268	0.0342	0.0538

IV. Conclusion

A novel integrated 4-element MIMO antenna system for 4G/5G mobile applications was successfully simulated and fabricated. The proposed design is low profile, compact and simple (consisting of a single substrate) and provides 2-element MIMO system for each standard. The integrated antenna system is multi-band and covered 1975-2080 MHz, 2160-2230 MHz, 2350-2620 MHz, 3060-3140 MHz and 3480-3540 MHz for 4G bands and 16.50-17.80 GHz band for 5G. MIMO performance metrics were calculated with high gain and good efficiency values. Good agreement between simulated and measured results was obtained.

References

[1] M. S. Sharawi, *Printed MIMO Antenna Engineering*, MA: Artech House, Norwood, 2014.

[2] J. G. Andrews, S. Buzzi, W. Choi, S. V. Hanly, A. Lozano, A. C. K. Soong, and J. C. Zhang, ''What will 5G be ?,'' IEEE journal on selected areas in communications, vol. 32, no. 6, pp. 1065–1082, June 2014.

[3] L. Yang and T. Li, ''Box-folded four-element MIMO antenna system for LTE handsets,'' IET Journals & Magazines, vol. 51, no. 6, pp. 440–441, March 2015.

[4] L. Yang and T. Li, ''G. Li, H. Zhai, Z. Ma, C. Liang, R. Yu, and S. Liu,''Isolation-Improved Dual-Band MIMO Antenna Array for LTE/WiMAX Mobile Terminals,''IEEE Antennas and Wireless Propagation Letters, vol. 13, pp. 1128–1131, 2014.

[5] Y. Yao, X. Wang, and J. Yu, ''Multiband Planar Monopole Antenna for LTE MIMO Systems,''International Journal of Antennas and Propagation, 2012.

[6] S. Shoaib, I. Shoaib, N. Shoaib, X. Chen, and C. G. Parini, ''Design and Performance Study of a Dual-Element Multiband Printed Monopole Antenna Array for MIMO Terminals,'' IEEE Antennas and wireless Propagation Letters, Vol. 13, pp. 329–332, 2014.

[7] S. C. Fernandez, and S. K. Sharma, ''Multiband Printed Meandered Loop Antennas With MIMO Implementations for Wireless Routers,'' IEEE Antennas and Wireless Propagation Letters, vol. 12, pp. 96–99, 2013.

[8] D. Sarkar, A. Singh, K. Saurav,and K. V.Srivastava, ''Four-element quad-band multiple-input–multiple-output antenna employing split-ring resonator and inter-digital capacitor,'' IET Microwaves, Antennas and Propagation, vol. 09, pp. 1453–1460, 2015.

[9] Andrea Neto, and J. J. Lee, ''Ultrawide-Band Properties of Long Slot Arrays,''IEEE Transaction on Antenna and Propagation, vol. 54, no. 2, pp. 534–543, Feb, 2006.

[10] A. Neto, D. Cavallo, G. Gerini, and G. Toso, ''Scanning Performances of Wideband Connected Arrays in the Presence of a Backing Reflector,''IEEE Transaction on Antenna and Propagation, vol. 57, no. 10, pp. 3092–3102, Oct. 2009.

[11] D. Cavallo, A. Neto, G. Gerini, A. Micco, and V. Galdi, ''A 3-to 5-GHz Wideband Array of Connected Dipoles With Low Cross Polarization and Wide-Scan Capabilities,''IEEE Transaction on Antennas and Propagation, vol. 61, no. 3, pp. 1148–1154, March 2013.

[12] J. Gilmore; D. B. Davidson, ''Suppressing Undesired Common-Mode Resonances in Connected Antenna Arrays,''IEEE Transactions on Antennas and Propagation, vol. 53, pp. 5245–5250, 2015.

[13] H. B. Molina, and J. Hesselbarth, ''Reactively Matched Long Slot Linear Connected Array Antenna,''IEEE 9th European Conference on Antennas and Propagation (EuCAP), pp. 1–5, 2015.

[14] J. J. Lee, S. Livingston, and R. Koenig, ''Wide Band Long Slot Array Antennas,''IEEE International Symposium on Antennas and Propagation Society, pp. 452–455, 2003.

[15] S.-T. Liu, Y.-W. Hsu, and Y.-C. Lin, ''A Dual Polarized Cavity-Backed Aperture Antenna for 5G mm W MIMO Applications,'' IEEE International Conference on Microwaves, Communications, Antennas and Electronic Systems (2015), Tel Aviv, Israel, Nov. 2015.

[16] O. M. Haraz, M. Ashraf, and S. Alshebeili, ''Single-Band PIFA MIMO Antenna System Design for Future 5G Wireless Communication Applications,'' IEEE 11th International Conference on Wireless and Mobile Computing, Networking and Communications (WiMob), pp. 608–612, 2015.

[17] A. T. Alreshaid, M. S. Sharawi, S. Podilchak, and K. Sarabandi, ''Compact millimeter-wave switched-beam antenna arrays for short range communications,'' Microwave and optical technology letters, Wiley, vol. 58, no. 8, pp. 1917–1921, Aug 2016.

[18] Y.-L. Bani, C. Li, C.-Y.-D. Sim, G. Wu, and K.-L. Wong, ''4G/5G Multiple Antennas for Future Multi-Mode Smartphone Applications,'' IEEE Journals and Magazines, vol. 4, pp. 2981–2988, June 2016.

[19] Z. Qin, W. Geyi, M. Zhang, and Jun Wang, ''Printed eight-element MIMO system for compact and thin 5G mobile handest,'' IET Journals & Magazines, vol. 52, no. 6, pp. 416–418, March 2016.